UNIVERSITY *of York*

This is a repository copy of *Power loss and hotspot analysis for photovoltaic modules affected by potential induced degradation*.

White Rose Research Online URL for this paper:
https://eprints.whiterose.ac.uk/id/eprint/183245/

Version: Published Version

Article:

White Rose
university consortium
Universities of Leeds, Sheffield & York

eprints@whiterose.ac.uk
https://eprints.whiterose.ac.uk/

ARTICLE   OPEN

Check for updates

Power loss and hotspot analysis for photovoltaic modules affected by potential induced degradation

Mahmoud Dhimish [1]✉ and Andy M. Tyrrell[1]

Potential-induced degradation (PID) of photovoltaic (PV) modules is one of the most severe types of degradation in modern modules, where power losses depend on the strength of the electric field, the temperature and relative humidity, and the PV module materials. Previous studies have only considered single effects of PID; however, this work investigates the power losses, development of hotspots, mm-level defects, and the performance ratio (PR) of 28 PID affected PV modules. Following a standard PID experiment, it was found that (i) the average power loss is 25%, (ii) hotspots were developed in the modules with an increase in the surface temperature from 25 to 45 °C, (iii) 60% of the examined PV modules failed the reliability test following IEC61215 standard, and (iv) the mean PR ratio is equivalent to 71.16%.

INTRODUCTION

One of the most valuable characteristics of photovoltaic (PV) technology is its high stability, with potential operational lifetimes of over 30 years. Continuous developments from academic and industrial researchers to improve the PV efficiency and overcome manufacturing costs has contributed significantly to PV's success. In the wake of the accelerated growth of the PV industry, the reliability of PV technologies has recently caught considerable attention from researchers, manufacturers, and investors. Although PV modules have long been considered reliable under field conditions with low degradation and failure rates, they can be affected by diverse degradation mechanisms, which collectively reduce the module crop power over time. One of the main degradation mechanisms is called potential-inducted-degradation (PID)[1–3]. For many PV systems, PID is one of the leading causes of module degradation caused by the high voltage between the encapsulants and the front glass surface, which is grounded via the substructure of the cell or the frame[4].

PID becomes more prevailing as the module ages, and whilst it normally does not affect all the solar cells in the module, it does have a critical impact as it cannot be repaired[5]. For example, in recent studies[1,6], PV modules with different types of structure (poly/monocrystalline silicon) were subjected to PID experiments under the IEC61215 standard[7]. They explain that there are 8–30% power losses under standard test conditions. However, they do not consider the impact of varying the solar irradiance, temperature or analyzing the thermal behaviour in the PID tested PV modules.

Other researchers[8,9] have reported that cracks in solar cells can accelerate PID due to the localized heat caused by the cracks. This phenomenon happens when a crack is initiated in the cell; hence, nonuniform distribution of the current in the fingers and busbars transpires. Consequently, localized heating has been shown to develop, commonly known as hotspots. In contrast, there is little knowledge on the correlation between PID and the development of hotspots. From former research[10,11] it is understood that hotspots are likely to occur in PV installation, yet it is not fully understood as to whether PID impacted PV modules' hotspots and the potential increase in their temperature.

Other PV failure modes, including failure in the bypass diodes[12], permanent shading[13], or shunting (increase in the resistance of the cells)[14], have been identified as likely to accelerate PID. However, these failure modes are usually mitigated by utilising state-of-the-art power electronics devices[15,16], and they can be distinguished using mathematical and machine learning algorithms[17,18].

To identify the consequence of PID on PV modules, electro-luminescence (EL) imaging is usually performed[19–21]. For example, in Fig. 1, the EL image is shown for two different solar cells before and after the PID experiment was performed. The darker exhibition of the cells under EL testing corresponds to less efficiency, with an estimated power loss of −17% and −22%, respectively. However, other researchers[22,23] have suggested using photoluminescence (PL) imaging to consider the effects of PID on cells. PL imaging is more practical for inspecting large-scale PV modules. PL imaging cannot identify inactive areas in the cells, and the interconnection failure, whereas an EL imaging setup can identify both failure modes[24].

Former work on the PID effect on the performance of PV modules has been widely investigated using indoor experiments[25,26]. As a result, there is a lack of erudition on the behaviour of PV module affected by PID using long term data measurements. New examination techniques that would correlate with PID, such as humidity-induced degradation (HID)[27] temperature-induced degradation (TID) is of significant interest and can give useful information to help inform identification of hotspots[28]. However, performing HID or TID experiments requires a complicated experimental setup and advanced (high cost) climate chambers.

In this paper, we will present the results on investigating 28 PV modules affected by PID. The analysis will include the output power losses under varying solar irradiance, thermal behaviour and hotspots development, mm-level inspection, and the performance ratio of the PV modules over 12-months of field service. In addition, following the IEC61215 standard, we will discuss the reliability test for all examined modules.

---

[1]Department of Electronic Engineering, University of York, York, UK. ✉email: Mahmoud.dhimish@york.ac.uk
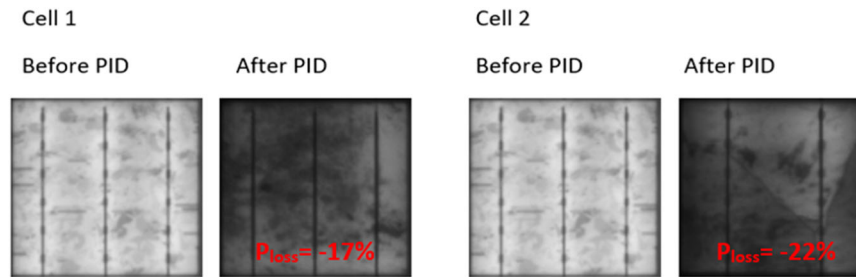
Fig. 1 EL images were taken before and after the PID test. The EL images are captured using Brightspot EL imaging setup, and the power loss (P_{loss}) was estimated under the standard test conditions.
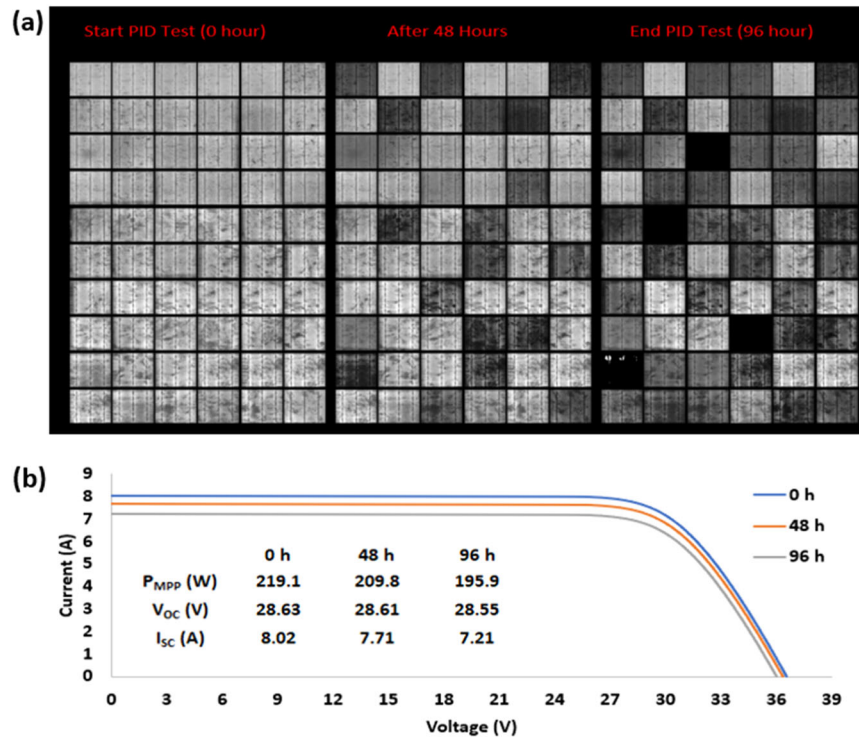

Fig. 2 Results of the PID test. a EL image of a PV module before and after the PID test is performed at 0, 48, and 96 h. **b** Measured I–V curves under the standard test conditions.
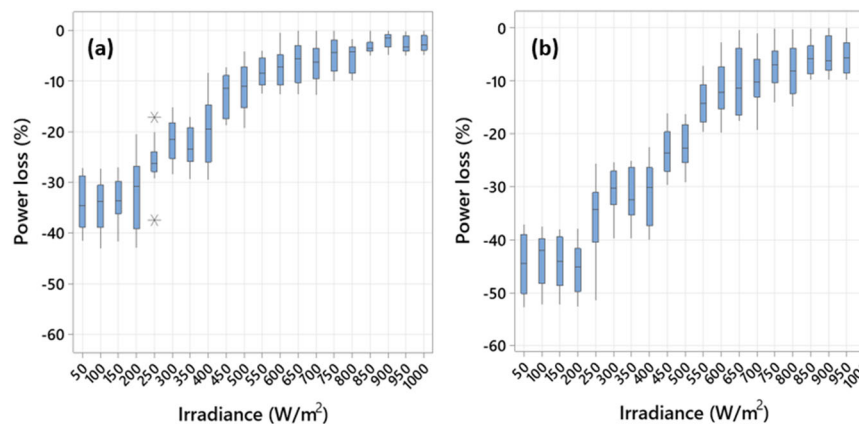

Fig. 3 Calculated power losses versus irradiance. a PID test at 48 h, **b** PID test at 96 h. The irradiance step change is 50 W/m² taken for the 24 tested PV modules, and the temperature is maintained at 25 °C. The error bars represent the average collected data of the 28 tested PV modules.
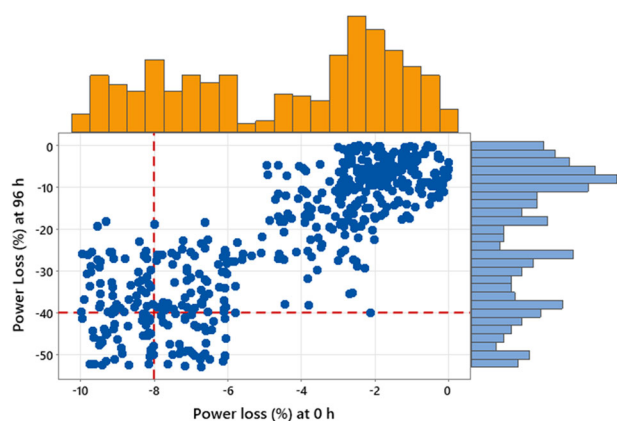
Fig. 4 Marginal plot of the samples taken during the PID test at 0 h and after 96 h. The histogram corresponds to the actual distribution of the data taken during both experiments, PID at 0 h and 96 h.

RESULTS AND DISCUSSIONS

PID testing

The PID tests were performed on the 28 tested PV modules. For example, Fig. 2a, shows the EL images of one of the examined PV modules at 0, 48, and 96 h. It is clear that the PID test develops a complete degradation mode for several cells, leading to a drop in the output power. Figure 2b shows the module's measured I–V curves; as time progresses, as can be seen from these graphs there is a significant drop in the output power. Using Eq. (1), the output power loss is equal to −10.58% after completing the PID testing. Consequently, there is a notable drop in the I_{SC}, however, there is only a slight change in the V_{OC}.

The V_{OC} slightly decreases as the module temperature increases. Accordingly, there is an expected increase in the module temperature after performing the PID testing. However, this increase is insufficient to drop the V_{OC} drastically. In comparison, a more significant drop in the I_{SC} is distinguished because the short-circuit drops when several factors change, such as a decrease in the solar cell area (i.e., cracks development in the cell) and a reduction of the number of photons observed by the cells.

For all tested PV modules, the correlation between the measured power losses vs irradiance during the PID test at 48 and 96 h were measured (Fig. 3), the values at 0 h have not been considered as the power losses are minimal. The power losses at 50–200 W/m^2 is 2–4 times higher than at 1000 W/m^2. This effect is due to shunting, which increases while irradiance levels are decreasing. This result concurs with the scientific community, where the PID is closely associated with reducing shunt resistance[29,30]. A marginal plot is a scatterplot that compares two different experiments using the data samples histogram. Accordingly, a marginal plot has been obtained and demonstrated in Fig. 4 using the measurements of the PID experiment at the initial state (0 h) and by the end of the experiment (96 h). The x-axis and y-axis represent the power losses of the examined PV module at 0 and 96 h, respectively.

The results confirm a significant power loss in the examined PV module after being subjected to the PID test for 96 h. For example, if a PV module has −8% power losses at the initial state of the PID test, the power losses would likely be in the range of −30% ~ −50% after 96 h.

This study has considered the cumulative density function (CDF) of all measured samples, as shown in Fig. 5. This plot gives an indication of the PID impact over time. The y-axis represents the percentage of the PV module performing a specific power loss. For example, after 48 and 96 h of PID testing, there is a 50% chance that the power loss of the PV module is −14.97% and −21.73%,
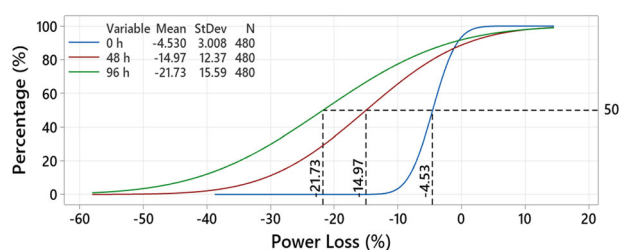

Fig. 5 Cumulative distribution function of all measured samples. The horizontal dashed line at 50% corresponds to the mid-range of the percentile.
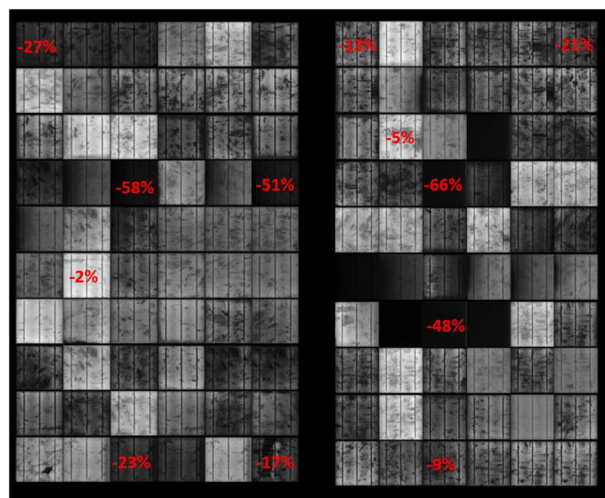

Fig. 6 EL images after PID are completed for two different PV modules. The power loss labelled in red was estimated under the standard test conditions.

respectively. On the other hand, there is only −4.53% power loss before the PV module is affected by PID (at 0 h). It is worth noting here that 50% has been applied as it corresponds to the mid-range of the percentile, which provides a more accurate prediction of the power losses.

The correlation between the EL images and the actual power losses of the solar cells is shown in Fig. 6. Both PV modules EL images were taken after the PID was completed, at 96 h. This feature is already available using the EL software. It uses the difference in the light/spectrum of non-PID versus the PID images; hence, the power losses can be estimated. The "blackout" EL images does not necessarily resemble −100% losses in the output power. This is because they have no illumination under the EL test; however, they still generate current. In contrast, it is relevant to reflect that few solar cells are unaffected after completing the PID test, and their output power losses remain below −5%. This suggests that these cells were influenced by lower shading rates, heat, humidity, or any form of cracks during their working life.

The correlation between the PID and the increase in the temperature of the solar cell has also been investigated. Figure 7 shows that at the start of the PID test, 0 h, the surface temperature of the PV module is approximately 22 °C. After 48 h of PID testing, the PV modules develop nearly 20 hotspots with an increased temperature varying from 25 to 30 °C. At 96 h, the PID experiment has impacted the PV module with 30 hotspots, with four being affected by a significant increase in the temperature, 45 °C. The development of these hotspots will now affect the reliability and durability of the PV modules, making them less efficient and more difficult to operate than before the PID test.
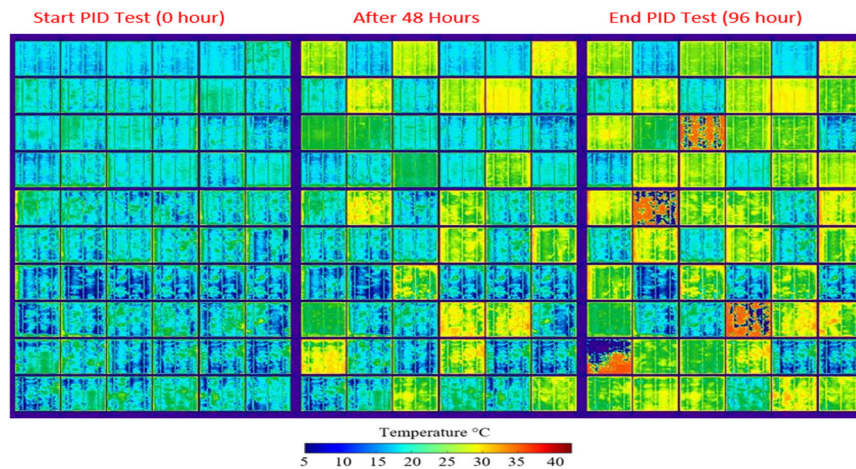
Fig. 7 Thermal images for one of the examined PV modules taken under standard test conditions. The EL image of this PV module is shown in Fig. 2.
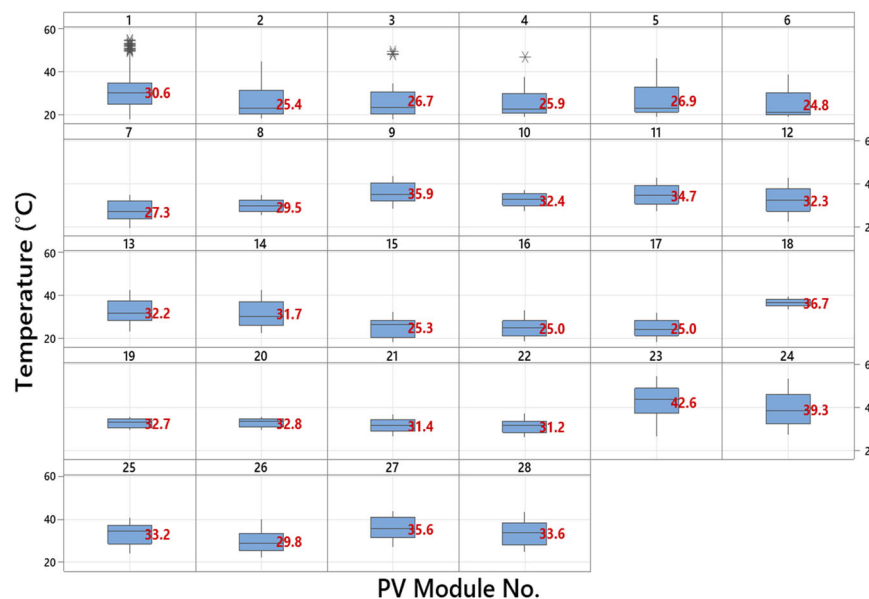

Fig. 8 Extracted PV modules temperature after PID test was performed. The error bars represent the collected data of the 28 tested PV modules after completing a single PID test (96 h).

Observing the evolution of the hotspots and considering the average surface temperature in the PV module, it can be observed that an increase in the PV module temperature after the PID test is likely to follow. It is also expected that multiple hotspots are being created in the module. The resultant hotspots in the module will impact the yield power, therefore, and as illustrated in Fig. 3, the power loss of the modules affected after the PID is completed can vary depending on the solar illumination, but, on average, there is −25% drop in the output power.

According to Fig. 7, some solar cells are affected by a significant increase in their temperature, up to 40 °C. This is because these cells are generating a much lower current compared with adjacent cells. Usually, this phenomenon occurs when the cells are being affected by cracks.

Using FLIR software, the temperature data from all the PV modules after completing a single PID test (96 h) can be extracted; the temperature profile are presented in Fig. 8. The mean value of the PV modules temperature varies between 25 to 42 °C. Therefore, following the IEC61215 standard, if the average PV temperature is above 30 °C, it is assumed that the PV module fails the reliability test. In contrast, and according to the results

illustrated in Fig. 8, it can be recognized that 17 out of the 28 examined PV modules fail the reliability test. Therefore, these modules are likely to have severe degradation when exposed to environmental/outdoor conditions.

Cell level PID affect

The PID can develop three principal defects in solar cells: cracks, blackout, or central or central breakdown area (Table 1). The first principal defect caused by PID is the development of cracks, or what is well known as microcracks (μcracks)[31]. This defect type can influence the output power generation of the solar sample, but it is unlikely to impact the cell with a hotspot. For example, in Table 1, it is evident that there is no increase in the surface temperature of the first solar cell sample, which is affected by cracks.

However, hotspots developed in the cells affected by the other two types of defects, blackout, and central breakdown area, which caused an increase in the cells surfaces temperature from 25 °C to approximately 40 °C. Here an inhomogeneous distribution of the solar irradiance and uneven flow of the current in the busbars would typically cause an irregular distribution of the heat across
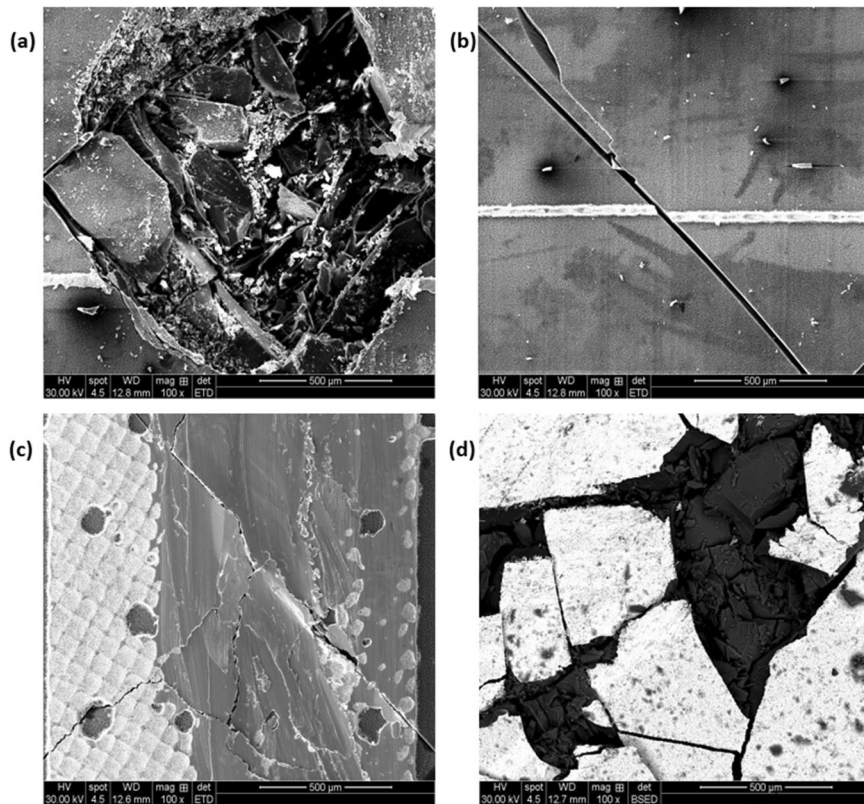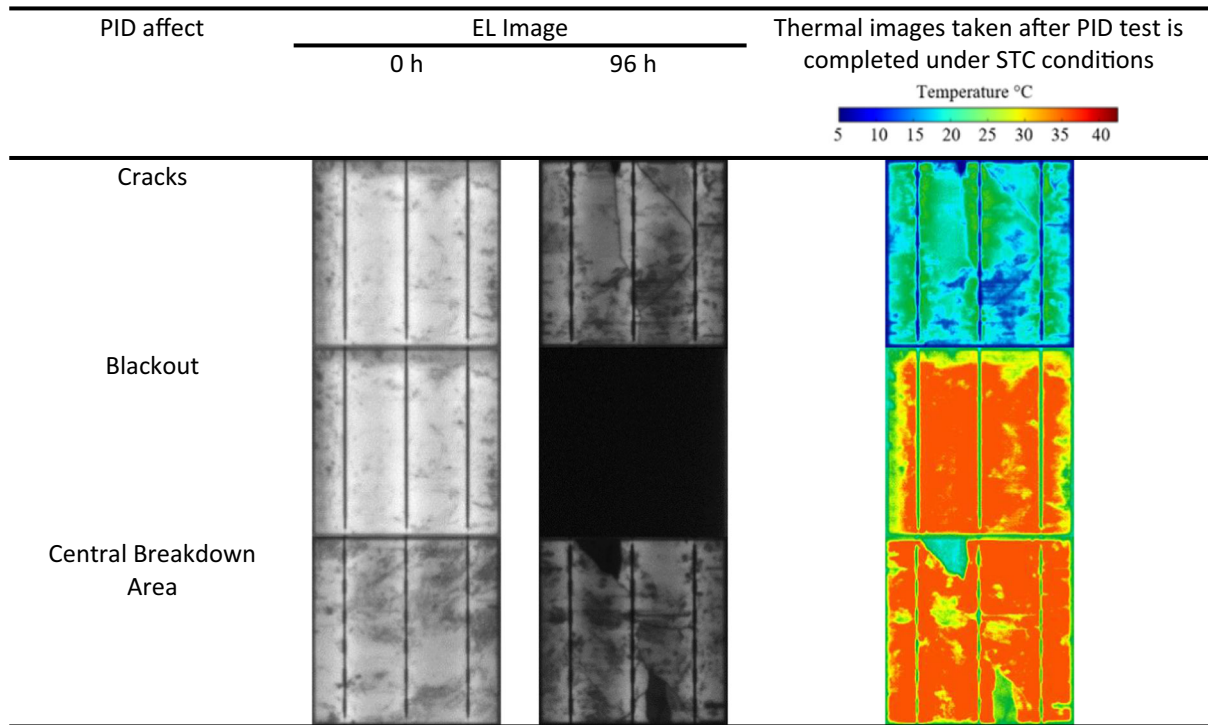
Table 1. Cell-level PID affect.

| PID affect	EL Image		Thermal images taken after PID test is completed under STC conditions
	0 h	96 h	Temperature °C 5 10 15 20 25 30 35 40
Cracks			
Blackout			
Central Breakdown Area			

Fig. 9 SEM images of four different solar cell samples. a Breakdown in the surface. **b** Discontinuity in the cell finger. **c** Discontinuity in the cell busbar. **d** Breakdown in the back sheet of the solar cell.

Table 2. Electrical parameters of the examined PV modules at STC conditions.

Parameter	Value
Power at maximum power point (P_{MPP})	220 W
Current at maximum power point (I_{MPP})	7.68 A
Voltage at maximum power point (V_{MPP})	28.65 V
Short circuit current (I_{SC})	8.10 A
Open circuit voltage (V_{OC})	36.6 V
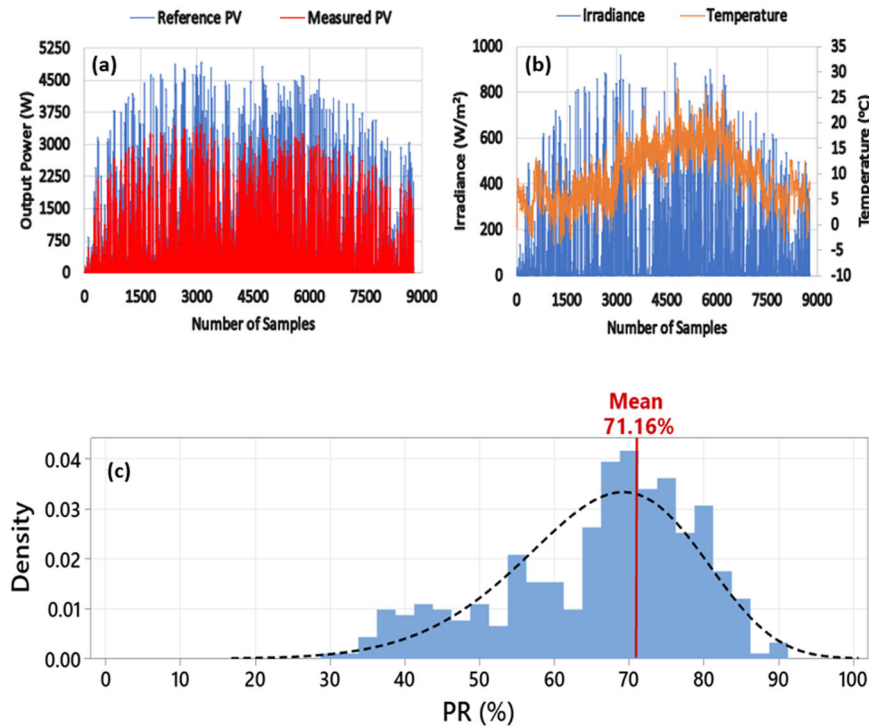
Fig. 10 Output measurements of the PV modules while operating in the field. a Measured PV output power (after PID test is completed) versus reference PV cell output power. **b** Solar irradiance and PV cell temperature. **c** PR ratio analysis.
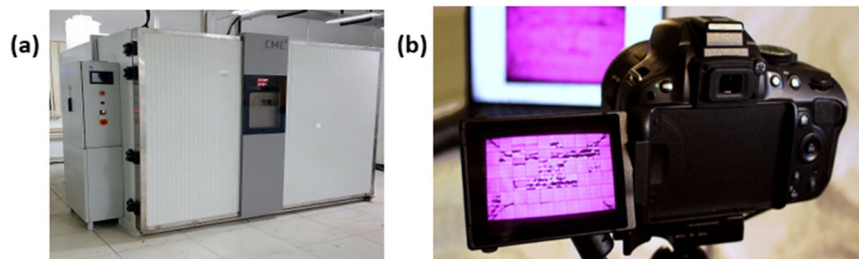
Fig. 11 PV testing equipment. a Damp heat test chamber. **b** EL imaging camera.

the solar cell surface. Following this, it is expected that hotspots develop in these affected cells. In addition, the output power losses due to blackout defects and central breakdown areas are much higher than the cracks, reasonably because more area in the cell has been damaged.

Furthermore, multiple solar cell samples under the Quanta FEC250 scanning electron microscope (SEM) were considered. These samples were subjected to the same PID test. The SEM is interfaced with a personal computer for data acquisition. The Back Scattered (Everhart-Thornley detector (ETD)) was selected to observe the impact of the PID on the solar cell samples.

It is observed that the PID impacted the cells through different types of mm-level defects. Figure 9 illustrates the four different kinds of defects caused by the PID. Figure 9a shows a breakdown area in the cell; this typically corresponds to a blackout region in the original EL image. Figure 9b, c presents the solar cell finger and busbar discontinuation, respectively. This is the root cause why PID-affected solar cells cannot generate a maximum current. In addition, the examination of the backside (back sheet) for a solar cell impacted by PID is shown in Fig. 9d. It is recognised that the back sheet is affected by breakdown areas; as a result, this would cause water vapour to enter the cell and degrade its performance.

Fig. 12 Examined PV modules placed outdoor after the PID test is completed. The PV system consists of 28 modules distributed among two strings, each string comprising 14 modules.

Performance ratio analysis

After the PID tests were performed, the PV modules were placed outdoors to monitor their performance. The PV modules were randomly selected and combined in two strings, each string comprising 12 series-connected modules. On the monitoring side, an inverter (SMA Sunny Tripower 15000TL-30) was used to connect the PV installation to the power grid and act as data acquisition for the system. To estimate the PR ratio using Eq. (2), the reference solar cell to evaluate the P_{STC} is required, and Davis weather station to measure G_{poa} and T_{ref}.

The output measured power versus the reference PV cell power is shown in Fig. 10a. In addition, Fig. 10b, presents the actual irradiance and temperature of the PV system. The data has been collected over 12-months. The PR is then calculated using Eq. (2), and as shown in Fig. 10c, the mean PR ratio is found at 71.16%.

According to the latest study on the examination of 3000 PV modules across the UK, it was discovered that the PR ratio varies from 83 to 88%[32]. Compared with these findings, the PR ratio of the test PV system is significantly low as the PV modules that were subjected to the PID experiment. This result proves that PV modules affected by PID degrade their performance under STC conditions and can severely impact their power production if placed outdoors.

In summary, this work reports the effect of PID on the performance of solar cells. We have applied the PID test on 28 PV modules and analysed their performance. First, we have discovered that after 96 h of PID testing, the power losses of the PV modules at lower irradiance levels (50–200 W/m^2) are approximately 2–4 times higher than at 1000 W/m^2. Then we have evidence that solar cells attacked by PID can develop hotspots, increasing the temperature of the cells from 25 °C to 45 °C. Following the IEC61215 standard we found 60% of the examined PV modules failed the reliability test after completing the PID experiment. In addition, on a mm-level, we have discovered that PID can impact the solar cells with different damages, such as discontinuation of the cells fingers and busbars. Finally, the PV modules were placed outdoors after the PID experiment was completed and determined that the mean PR ratio is 71.16%.

Our results can benefit the PV industry to understand how PID can influence the thermal and electrical performance of PV modules. In the future, we intend to establish considerable effort into exploring the design and implementation of PID prevention techniques and investigating different materials for mitigating this problem.

METHODS
PV modules characteristics

For experimental work presented in this paper, 28 PV modules, p-type polycrystalline silicon were tested. The PV modules' electrical parameters are presented in Table 2, taken at standard test conditions (STC), where the solar irradiance is 1000 W/m^2, and PV cell temperature is 25 °C.

PV testing procedure

The modules were placed in a damp heat test chamber (Fig. 11a) at 85% relative humidity and 85 °C and biased with a voltage of −1000 V. For the accelerated PID test, aluminium foil was placed on the front surface of the samples and kept in place with a glass plate. The positive and negative module contacts were shorted and connected to the negative terminal of a high-voltage power source. The Al foil was connected to the positive terminal. Following the IEC62804 standard, the EL images and current-voltage (I–V) curves were measured at 0, 48, 96 h. The relative power loss due to PID is then calculated using Eq. (1).

$$Power\ Loss = \frac{P_{MPP\ at\ 96\ hours} - P_{MPP\ at\ 0\ hours}}{P_{MPP\ at\ 0\ hours}} \times 100\% \tag{1}$$

where $P_{MPP\ at\ 96\ h}$ is the module maximum output power at the end of the PID testing, whereas $P_{MPP\ at\ 0\ h}$ is the module initial maximum output power.

The PVA-1500V3 PV analyzer kit was used to obtain the measurements for the I–V curves. This instrument can measure voltage up to 1500 V, and its I–V curve measurement precision is approximately ±2%. The Brightspot automation EL imaging setup (Fig. 11b) was used to capture the EL images of the PV modules. The EL imaging setup was not corrected over time to avoid altering the resolution of the EL captured images, even when the EL signal of several degraded modules dropped significantly.

After the PID test was completed, the examined PV modules were placed outdoor (Fig. 12) to analyse their performance ratio and whether any module would develop hotspots. The performance ratio was calculated over 12-months using Eq. (2), and for the thermal imaging inspection, a FLIR E54 thermal camera with thermal sensitivity of ±0.1 °C was utilised.

$$PR = \frac{P_{MEASURED}}{P_{STC} \frac{G_{poa}}{G_{ref}} \left(1 + \gamma(T_{PV} - T_{ref})\right)} \tag{2}$$

Related to (2) $P_{MEASURED}$ is the measured output power of the PV string in watts, P_{STC} is the rated power of the PV string in watts, G_{poa} is the plane-of-array irradiance, G_{ref} is the reference irradiance at STC condition 1000 W/m^2, γ is the temperature coefficient of the maximum power −0.34%/ °C, T_{PV} is the PV cell temperature in °C (Fig. 7b), and T_{ref} is the PV string reference temperature at STC condition 25 °C. The solar irradiance and PV cell temperature were taken using a weather station (Davis weather station). The precision of the solar irradiance and PV cell temperature was ±2 W/m^2 and ±0.5 °C, respectively.

REFERENCES
1. Bedrich, K. G. et al. Quantitative electroluminescence imaging analysis for performance estimation of PID-influenced PV modules. *IEEE J. Photovolt.* **8**, 1281–1288 (2018).
2. Carolus, J. et al. Why and how to adapt PID testing for bifacial PV modules? *Prog. Photovolt.* **28**, 1045–1053 (2020).
3. Zhang, J. W. et al. "Research on potential induced degradation (PID) of polymeric backsheet in PV modules after salt-mist exposure.". *Sol. Energy* **188**, 475–482 (2019).
4. Hylský, J. et al. "Effect of negative potential on the extent of PID degradation in photovoltaic power plant in a real operation mode.". *Microelectron. Reliab.* **85**, 12–18 (2018).
5. Annigoni, E., Virtuani, A., Sculati-Meillaud, F. & Ballif, C. Modeling potential-induced degradation (PID) of field-exposed crystalline silicon solar PV modules: focus on a regeneration term. *2017 IEEE 44th Photovoltaic Specialist Conference (PVSC)*, 2017.
6. Oh, W. et al. Field degradation prediction of potential induced degradation of the crystalline silicon photovoltaic modules based on accelerated test and climatic data. *Microelectron. Reliab.* **76**, 596–600 (2017).

7. Mei, A. et al. Stabilizing perovskite solar cells to IEC61215: 2016 standards with over 9,000-h operational tracking. *Joule* **4**, 2646–2660 (2020).

8. Dhimish, M., d'Alessandro, V. & Daliento, S. Investigating the impact of cracks on solar cells performance: analysis based on nonuniform and uniform crack distributions. *IEEE Trans. Ind. Inform.* **18**, 1684–1693 (2021).

9. Dong, N. C., Islam, M. A., Ishikawa, Y. & Uraoka, Y. The influence of sodium ions decorated micro-cracks on the evolution of potential induced degradation in p-type crystalline silicon solar cells. *Sol. Energy* **174**, 1–6 (2018).

10. Gomez-Vidal, J. C. Corrosion resistance of MCrAlX coatings in a molten chloride for thermal storage in concentrating solar power applications. *NPJ Mater. Degrad.* **1**, 1–9 (2017).

11. Qian, J., Thomson, A. F., Wu, Y., Weber, K. J. & Blakers, A. W. Impact of perovskite/silicon tandem module design on hot-spot temperature. *ACS Appl. Energy Mater.* **1**, 3025–3029 (2018).

12. Dhimish, M. & Chen, Z. Novel open-circuit photovoltaic bypass diode fault detection algorithm. *IEEE J. Photovolt.* **9**, 1819–1827 (2019).

13. Ghanbari, T. Permanent partial shading detection for protection of photovoltaic panels against hot spotting. *IET Renew. Power Gener.* **11**, 123–131 (2017).

14. Avenel, C., Raccurt, O., Gardette, J. L. & Therias, S. Accelerated aging test modeling applied to solar mirrors. *NPJ Mater. Degrad.* **3**, 1–14 (2019).

15. Olalla, C., Hasan, M., Deline, C. & Maksimović, D. Mitigation of hot-spots in photovoltaic systems using distributed power electronics. *Energies* **11**, 726 (2018).

16. Dhimish, M. 70% decrease of hot-spotted photovoltaic modules output power loss using novel MPPT algorithm. *IEEE Trans. Circuits Syst. II Express Briefs* **66**, 2027–2031 (2019).

17. Garoudja, E., Chouder, A., Kara, K. & Silvestre, S. An enhanced machine learning based approach for failures detection and diagnosis of PV systems. *Energy Convers. Manag.* **151**, 496–513 (2017).

18. Hussain, M., Dhimish, M., Titarenko, S. & Mather, P. Artificial neural network based photovoltaic fault detection algorithm integrating two bi-directional input parameters. *Renew. Energy* **155**, 1272–1292 (2020).

19. Chen, S. et al. Thorough subcells diagnosis in a multi-junction solar cell via absolute electroluminescence-efficiency measurements. *Sci. Rep.* **5**, 1–6 (2015).

20. Jiang, X. et al. Ultra-high open-circuit voltage of tin perovskite solar cells via an electron transporting layer design. *Nat. Commun.* **11**, 1–7 (2020).

21. Rai, M., Wong, L. H. & Etgar, L. Effect of perovskite thickness on electroluminescence and solar cell conversion efficiency. *J. Phys. Chem. Lett.* **11**, 8189–8194 (2020).

22. Doll, B. et al. Photoluminescence for defect detection on full-sized photovoltaic modules. *IEEE J. Photovolt.* **11**, 1419–1429 (2021).

23. Tex, D. M., Imaizumi, M. & Kanemitsu, Y. Analyzing the electrical performance of a solar cell with time-resolved photoluminescence: methodology for fast optical screening. *Phys. Rev. Appl.* **7**, 014019 (2017).

24. Kirchartz, T., Márquez, J. A., Stolterfoht, M. & Unold, T. Photoluminescence-based characterization of halide perovskites for photovoltaics. *Adv. Energy Mater.* **10**, 1904134 (2020).

25. Hasan, A. A. et al. Delamination-and electromigration-related failures in solar panels—a review. *Sustainability* **13**, 6882 (2021).

26. Luo, W. et al. Potential-induced degradation in photovoltaic modules: a critical review. *Energy Environ. Sci.* **10**, 43–68 (2017).

27. Yun, J. S. et al. Humidity-induced degradation via grain boundaries of HC (NH2)2PbI3 planar perovskite solar cells. *Adv. Funct. Mater.* **28**, 1705363 (2018).

28. Dupuis, J. et al. Light-and elevated temperature-induced degradation impact on bifacial modules using accelerated aging tests, electroluminescence, and photovoltaic plant modeling. *Prog. Photovolt.* **29**, 694–704 (2021).

29. Yamaguchi, S., Yamamoto, C., Ohdaira, K. & Masuda, A. Reduction in the short-circuit current density of silicon heterojunction photovoltaic modules subjected to potential-induced degradation tests. *Sol. Energy Mater. Sol. Cells* **161**, 439–443 (2017).

30. Yamaguchi, S., Yamamoto, C., Ohdaira, K. & Masuda, A. Comprehensive study of potential-induced degradation in silicon heterojunction photovoltaic cell modules. *Prog. Photovolt.* **26**, 697–708 (2018).

31. Bdour, M., Dalala, Z., Al-Addous, M., Radaideh, A. & Al-Sadi, A. A comprehensive evaluation on types of microcracks and possible effects on power degradation in photovoltaic solar panels. *Sustainability* **12**, 6416 (2020).

32. Dhimish, M., Schofield, N. & Attya, A. Insights on the degradation and performance of 3000 photovoltaic installations of various technologies across the United Kingdom. *IEEE Trans. Ind. Inform.* **17**, 5919–5926 (2020).

ACKNOWLEDGEMENTS

AUTHOR CONTRIBUTIONS

Both authors discussed the organization and the content of the manuscript. M.D. performed the experiments, prepared figures, and wrote the main manuscript text. A.M.T. validated the experimental results and revised the manuscript. Both authors have approved the manuscript before submission.

COMPETING INTERESTS

The author declares no competing interests.

ADDITIONAL INFORMATION

Correspondence and requests for materials should be addressed to Mahmoud Dhimish.

Reprints and permission information is available at http://www.nature.com/reprints

Publisher's note Springer Nature remains neutral with regard to jurisdictional claims in published maps and institutional affiliations.